DEVELOPMENT OF CONTROLLABLE FRICTION DAMPER USING HYDRAULIC SYSTEM DRIVEN BY GIANT MAGNETOSTRICTIVE ACTUATORS FOR SEMI-ACTIVE SEISMIC ISOLATION OF BUILDINGS

Eiji SATO[1] and Takafumi FUJITA[2]

ABSTRACT: A semi-active seismic isolation system with a controllable friction damper using piezoelectric actuators had been proposed to reduce response acceleration and displacement, compared with those of passive systems. However, it is difficult to apply this controllable friction damper to large structures because super-large piezoelectric actuators and large amplifiers are needed, since piezoelectric actuators press directly the friction materials. To solve this problem, this study has developed a new controllable friction damper using a hydraulic pump driven by giant magnetostrictive actuators. It is easy to enhance the capacity of the hydraulic system, so this new controllable friction damper can easily be applied to the large-scale semi-active seismic isolation structures. This paper outlines the results of the characterization experiments of the new controllable friction damper and excitation tests on the semi-active seismic isolation system using this damper.

Key Words: *Seismic Isolation, Semi-Active Control, Controllable Friction Damper Giant Magnetostrictive Actuators, Hydraulic system, Excitation Test*

INTRODUCTION

Several base-isolated buildings have been constructed using passive isolation systems to decrease response acceleration of superstructures during an earthquake. The trade-off is that large relative displacement is inevitable in the passive seismic isolation systems in order to decrease the response acceleration of the superstructures. Moreover, it is feared that when long-period earthquakes occur, a larger relative displacement will be generated for seismic isolation structures with long natural period.

We therefore developed a controllable friction damper using piezoelectric actuators for the semi-active seismic isolation building. In a previous research paper (Sato, 2005), we used excitation tests to confirm that the semi-active seismic isolation system with this controllable friction damper decreases response acceleration and relative displacement. The main mechanism of this controllable friction damper, is that the piezoelectric actuators directly control the pressure of the friction materials. However, using this controllable friction damper for large structures requires super large piezoelectric actuators and large capacity amplifiers. Therefore, it is difficult to realize the semi-active seismic isolation system for the large structures.

The present study developed a new controllable friction damper using a hydraulic system driven by giant magnetostrictive actuators to be applied to large structures. The generated displacement of the

[1] Cooperative Research Fellow
[2] Professor

giant magnetostrictive actuator is infinitesimal, but the generated force is large, and the response is very quick, as well as piezoelectric actuators. A hydraulic pump using the giant magnetostrictive actuators was developed to utilize these merits (Murata, 2000). The new controllable friction damper for the semi-active seismic isolation system was developed to apply a hydraulic brake system using this hydraulic pump. Normally, a response of the hydraulic brake system for vehicles is inadequate. However, the new controllable friction damper responds more quickly, using the hydraulic pump driven by the giant magnetostrictive actuators; therefore, this damper performs, used for the semi-active seismic isolation systems produces more satisfactory performances. Furthermore, a negative type brake (the oil pressure rises; therefore, the friction force falls) with a fail-safe was used in consideration of safety and reliability. The new controllable friction damper also effectively solves the problem of the seismic isolation structures swaying in the wind.

The hydraulic system's capacity easily enhance, so this new controllable friction damper can be effectively used with the large-scale structures.

This paper describes the details of the developed controllable friction damper. Characteristic tests examining the performances of the new controllable friction damper and excitation tests examining the performances of the semi-active seismic isolation system with the new controllable friction damper were conducted. The results of these tests are also described.

CONTROLLABLE FRICTION DAMPER

In a normal hydraulic brake system, a brake booster is built between a brake pedal and brake pads, and a large displacement is necessary for operating the brake pedal. The hydraulic system and the pneumatic system are combined to obtain a large force in railway brake systems, making the brake systems complex.

These brake systems have response and operational performance problems. As a result, the normal brake systems do not have adequate performance to be used as the controllable friction damper for semi-active seismic isolation systems.

In order to solve these problems, this study developed a new controllable friction damper with a new piston type hydraulic pump. The controllable friction damper consists of the main body and the hydraulic pump. The main body is shown in **Figure 1**. The main body consists of the brake, the rod,

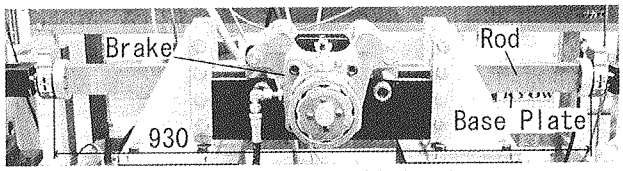

Figure 1 Controllable friction damper

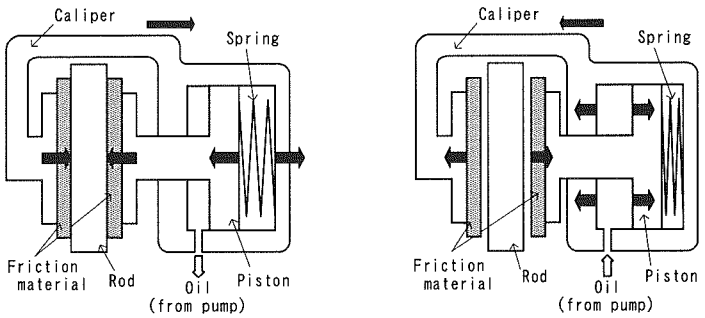

(a) Hold (b) Release

Figure 2 Schematic drawing negative brake

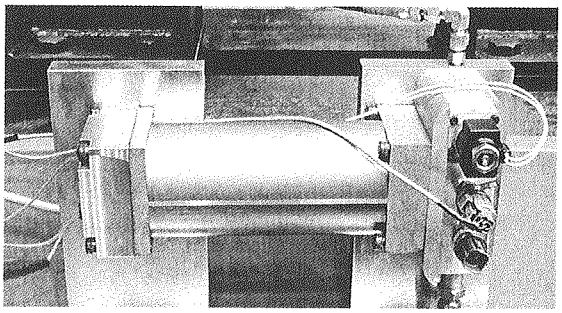

Figure 3 Hydraulic pump

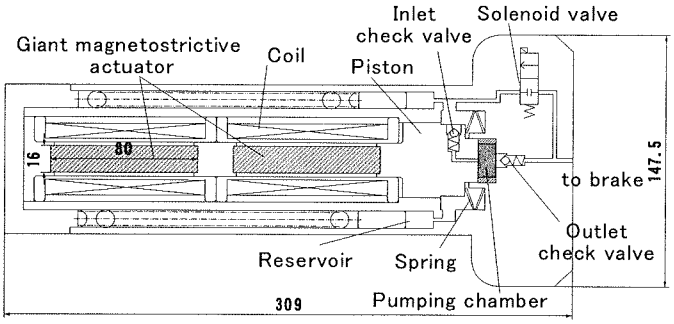

Figure 4 Plan of hydraulic pump

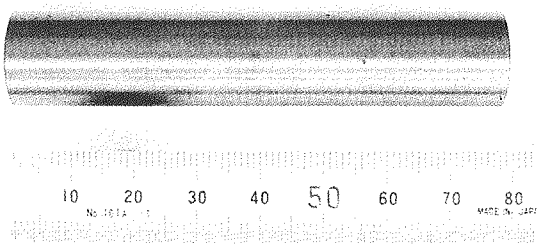

Figure 5 Giant magnetostrictive actuator

and the base plate. **Figure 2** depicts the mechanism of the brake. In the negative type brake, that the friction force is maximal to thrust the friction material with springs in normal circumstances. During an earthquake, the hydraulic pump increases the oil pressure. The force thrusting the friction material then falls, decreasing the friction force. The friction force can thus be varied by controlling the oil pressure using the hydraulic pump. If power fails and the controllable friction damper malfunctions during an earthquake, the negative brake prevents the controllable friction damper from producing a low friction force, thereby improving safety and reliability. Furthermore, the friction force is maximal in normal circumstances, solving the problem of the seismic isolation structure swaying in the wind.

The new hydraulic pump is presented in **Figure 3**, and the mechanism is depicted in **Figure 4**. The giant magnetostrictive actuators can be directly controlled and were built into the new piston type hydraulic pump. In this pump, the solenoid valve is closeded causing the pressure to rise. The piston then reciprocates with the use of the giant magnetostrictive actuators. Therefore, the oil pressure rises in the chamber due to the function of the check valves, and high-pressure oil is supplied to the brake. The solenoid valve is opened, and the oil pressure in the brake falls.

The giant magnetostrictive actuator is a magnetostrictive material alloy, which is magnetically elongated. **Figure 5** shows the giant magnetostrictive actuator, and **Table 1** presents the specifications.

Table 1 Specifications giant magnetostrictive actuator

Items	Specifications
Maker・Type	ETREMA・Terfenol-D
Nominal composition	Tb,Dy,Fe
Size	ϕ 16mm×80mm
Displacement	105 μ m
Force	7.9kN

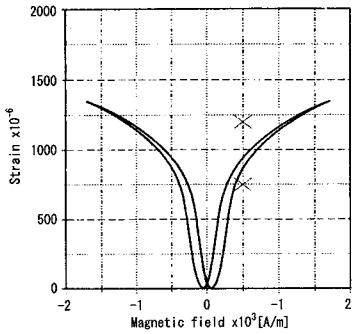

Figure 6 Relationship of magnetic field strength and strain

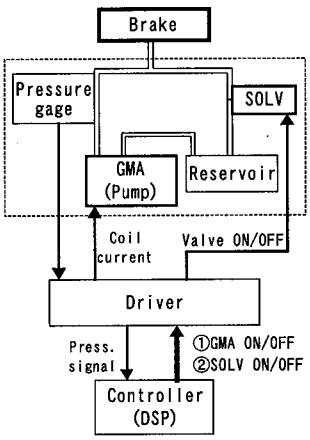

Figure 7 Configuration of controllable friction damper system

This actuator is 16 mm in diameter and 80 mm high. The present study used two actuators for the hydraulic pump. **Figure 6** illustrates the relationship between the magnetic field strength and the actuator strain. The generated displacement of the giant magnetostrictive actuator is infinitesimal, but the generated force is large, and the response is very quick, due to the solid actuator. As a result, the hydraulic pump's response and operational performance are improved.

Figure 7 depicts the system configuration of the controllable friction damper which is comprised of the brake, the hydraulic pump, and the control system. The hydraulic pump is connected with the driver, and various signals are transmitted. The controller (DSP) is connected with the driver and receives the oil pressure signal from the driver. The controller compares the measured oil pressure with the reference oil pressure, inputs the pressure increase signal (move the giant magnetostrictive actuator) or the pressure decrease signal (open the solenoid valve) to the driver, and controls the oil pressure. As a result, the high-pressure oil that is supplied from the pump to the brake varies the force thrusting the friction material, and the friction force can be varied.

CHARACTERISTIC EXPERIMENT OF CONTROLLABLE FRICTION DAMPER

Experimental Method

The controllable friction damper was excited by a hydraulic actuator and various data were collected to confirm the characteristics of this damper.

Experiment Result

Velocity Dependence Test Tests were conducted when the force thrusting the friction materials was constant to confirm that the friction force was not dependent on the sliding velocity. The controllable friction damper was excited with sinusoidal waves so that the maximum velocities generated by the hydraulic actuator were 5, 10, 15 and 20cm/s. **Figure 8** illustrates the hysteresis when the oil pressure of the controllable friction damper was 0.5 MPa. The hysteresis was the same at all velocities, confirming that the friction force was independent of the sliding velocity.

Response test Frequency response tests were conducted to confirm the response characteristics of the controllable friction damper. Sinusoidal waves whose frequency had been gradually swept, were used as the reference oil pressure; then the frequency response was calculated from the reference oil pressure and the friction force. These results are shown in **Figure 9**. The gain began to decrease at 2 Hz and decreased about 10dB at 13Hz. The phase had delays of about 16° at 2 Hz and about 90° at 13 Hz. The solid lines in these figures denote the identification results in the first-order lag. It is confirmed that these identification results almost agreed with these experiment results.

Friction Force Fluctuation Test The controllable friction damper was excited when the reference oil pressure was changed from 0MPa to 2MPa, confirming the relationship between the reference oil pressure and the generated friction force. This result is shown in **Figure 10**. The dashed line in this

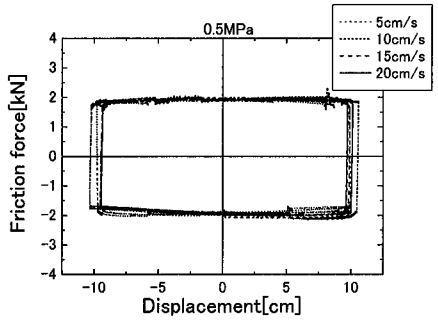

Figure 8 Hysteretic behavior (at 0.5MPa)

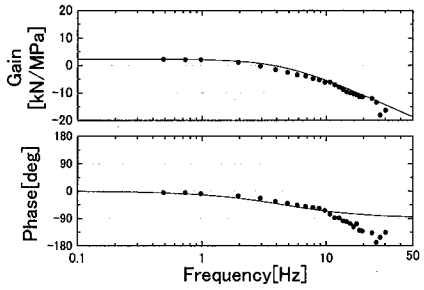

Figure 9 Frequency response characteristics

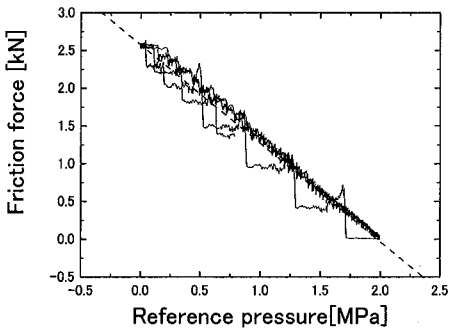

Figure 10 Relationship of reference pressure and friction force

figure denotes the function that was linearly approximated from the experiment results. Pulses of oil were generated as the solenoid valve was abruptly opened or closed; therefore, the friction force was turbulent. However, the approximated linear function nearly agreed with the experiment results.

FUNDAMENTAL ANALYSIS OF SEMI-ACTIVE SEISMIC ISOLATION SYSTEM WITH CONTROLLABLE FRICTION DAMPER

Analysis Model

Controllable Friction Damper An analysis model of the controllable friction damper was constructed from the characteristic experiment results. The relationship between the reference oil pressure and the generated friction force is modeled as follows.

$$u(t) = a + b \cdot p(t) \tag{1}$$

where $u(t)$ is the generation force (input), $p(t)$ is the reference oil pressure, and a and b are coefficients obtained from the experiments.

The delay of the controllable friction damper was modeled from the frequency response tests with the first-order lag as follows.

$$T_L \dot{f}(t) + f(t) = u(t) \tag{2}$$

where T_L is a time constant, and $f(t)$ is the generated friction force containing the delay of the controllable friction damper.

Seismic Isolation Structure Model The semi-active seismic isolation system with the controllable friction damper using the hydraulic system driven by the giant magnetostrictive actuators was modeled as a one-degree-of-freedom system to investigate semi-active controllers. This model's equation of motion is expressed in two phases, as indicated below, considering transition of static/dynamic friction due to the presence or absence of sliding at the friction damper.

Phase I : No sliding at the friction damper

$$\begin{cases} x = const. \\ \dot{x} = 0 \\ \ddot{x} = 0 \end{cases} \tag{3}$$

Phase II : Sliding at the friction damper

$$\ddot{x}(t) + 2\zeta\omega\dot{x}(t) + \omega^2 x(t) + \mathrm{sgn}\left(\dot{x}(t)\right)\frac{|f(t)|}{m} = -\ddot{z}(t) \tag{4}$$

where x is the relative displacement between the superstructure and the ground, ζ is the damping ratio, ω is the natural circular frequency of the isolation system, m is the mass of the superstructure, f is the controllable friction force, and $\ddot{z}$ is the earthquake wave acceleration.

The transition criteria between Phase I and Phase II are:

1) From Phase I to Phase II

$$|kx + m\ddot{z}| > f \tag{5}$$

2) From Phase II to Phase I

$$\dot{x} = 0 \quad \text{and} \quad |m\ddot{x}| < 2f \tag{6}$$

Semi-Active Seismic Isolation Control

Linear Quadratic Optimum Regulator Theory The optimal generation force is obtained by using Linear Quadratic (LQ) optimum regulator theory. When the controllable friction damper is used in a semi-active seismic isolation system, the equation of motion expressed by Equations (3) and (4) is nonlinear. Therefore, in this state, optimal input cannot be obtained by LQ. Thus, the friction force is considered to be the outside force $f'(t)$, and the equation of motion is made linear (Sato, 2005). The performance function J is defined as follows.

$$J = \int_0^\infty \left(\alpha \left(\ddot{x}(t) + \ddot{z}(t) \right)^2 + \beta x^2(t) + \gamma u^2(t) \right) dt \tag{7}$$

where α, β, and γ are weighting coefficients. When the state variable is $\mathbf{X}^T(t) = \left[x(t) \quad \dot{x}(t) \quad f'(t) \right]$, the linearized equation of motion transforms the state equation as follows with Equation (2) of the controllable friction damper model.

$$\dot{\mathbf{X}}(t) = \mathbf{A}\mathbf{X}(t) + \mathbf{B}u(t) + \mathbf{d}\ddot{z}(t) \tag{8}$$

The regulator problem is thus solved, and the optimal control input is obtained below.

$$u^*(t) = -\mathbf{F}_b \mathbf{X}(t), \quad \mathbf{F}_b = \mathbf{R}^{-1}\mathbf{B}^T\mathbf{P} \tag{9}$$

where $\mathbf{P}$ is the solution obtained from Riccati algebraic equation as follows.

$$\mathbf{P}\mathbf{A} + \mathbf{A}^T\mathbf{P} - \mathbf{P}\mathbf{B}\mathbf{R}^{-1}\mathbf{B}^T\mathbf{P} + \mathbf{Q} = 0 \tag{10}$$

where $\mathbf{R}$ and $\mathbf{Q}$ are the weighting matrices of the quadratic form performance function calculated from Equations (7) and (8).

Finally, the semi-active seismic isolation condition is used. The friction force was initially considered to be the outside force; however, the friction damper cannot generate the force in the same direction as the relative velocity. Therefore, the optimal control input was obtained.

$$u(t) = \begin{cases} u^*(t) & u^*(t) \cdot \dot{x}(t) \geqq 0 \\ 0 & u^*(t) \cdot \dot{x}(t) < 0 \end{cases} \tag{11}$$

Instantaneous Optimal Control Instantaneous Optimal Control (IOC) is effective in a nonlinear system (Yang, 1975). Therefore, although the equation of motion of the semi-active seismic isolation system with the controllable friction damper is nonlinear, the controller can be designed with IOC. The performance function $J(t)$ of IOC is defined as follows.

$$J(t) = q_v \dot{x}^2(t) + q_d x^2(t) + u^2(t) \tag{12}$$

where q_v, and q_d are weighting coefficients.

Lagrange method of undetermined multipliers is used to minimize the performance function $J(t)$.

Therefore, the optimal control input $u^*(t)$ is obtained as follows.

$$u^*(t) = \frac{q_v \Delta t^2 \operatorname{sgn}\left(\dot{x}(t)\right)}{2m\left(2T_L + \Delta t\right)\left(1 + \frac{\Delta t^2}{6}\omega^2 + \Delta t\zeta\omega\right)}\dot{x}(t) + \frac{q_d \Delta t^3 \operatorname{sgn}\left(\dot{x}(t)\right)}{6m\left(2T_L + \Delta t\right)\left(1 + \frac{\Delta t^2}{6}\omega^2 + \Delta t\zeta\omega\right)}x(t) \qquad (13)$$

where Δt is the sampling time.

Numerical Simulation

Numerical simulations of the semi-active seismic isolation system with each control theory were conducted before shaking table tests, and various performances were examined.

The analytical model applied to the simulation was the one-degree-of-freedom system. The mass of the analytical model was 6,000 kg, the natural period was 3 s, and the damping ratio was 3 %. The input earthquake motion was El Centro NS (1940, Imperial Valley Earthquake). The velocity levels of the input waves were set to 25, 50, 75, and 100 cm/s.

Figures 11 and **12** illustrate the results of the simulations when the semi-active controllers were designed by LQ and IOC, respectively. The simulations were conducted with the controllers that were designed to reduce response acceleration (Acc. reduction) and relative displacement (Disp. reduction). For comparison, the results of the passive seismic isolation system with a linear damping factor of 20% are illustrated in these figures. The maximum acceleration of input waves is also illustrated in the results of the maximum response acceleration. The response acceleration of the semi-active seismic isolation system became less than a quarter of the maximum acceleration of the input wave. In the best-case scenario with LQ, the response acceleration was decreased to 10.6 % of the input

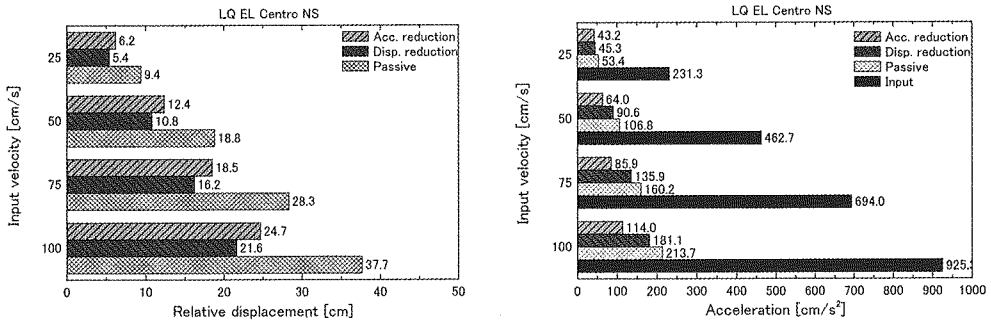

(a) Maximum response displacement (b) Maximum response acceleration

Figure 11 Simulation results for LQ

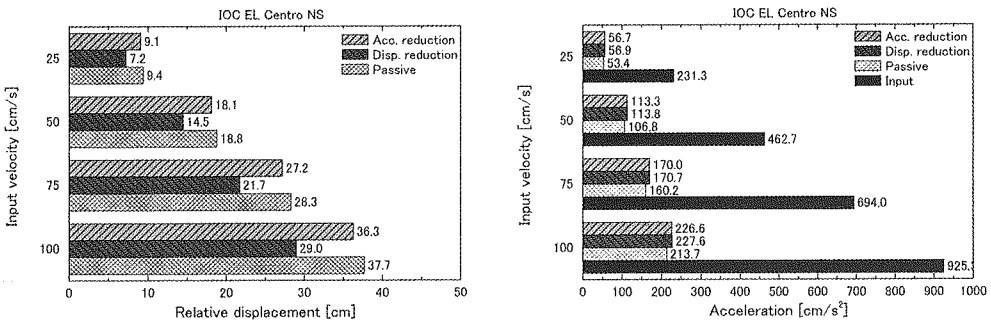

(a) Maximum response displacement (b) Maximum response acceleration

Figure 12 Simulation results for IOC

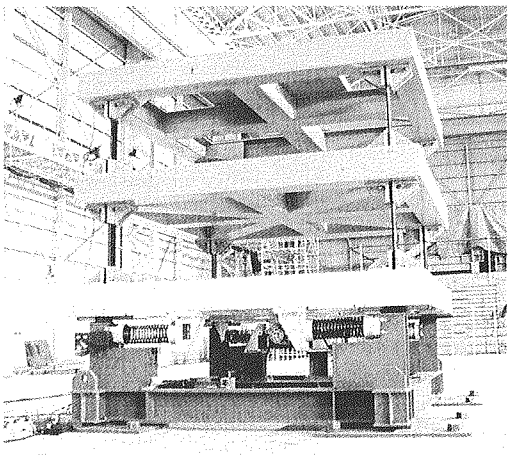

Figure 13 Test model

acceleration, and to 53.3 % of that of the passive seismic isolation system.

In the case of IOC, a high level seismic isolation performance was demonstrated, even though the response acceleration increased by 6 % to 7 % when compared to the results of the passive seismic isolation system. The relative displacement of all semi-active seismic isolation systems was less than that of the passive seismic isolation system. The displacement was significantly reduced when the controllers were designed to reduce the relative displacement by LQ and IOC. Compared to the passive seismic isolation system, in the best-case scenario with LQ, the relative displacement was decreased to 57.3 %. In the best-case scenario with IOC, the relative displacement was decreased to 75.4 %.

The seismic isolation performance of the semi-active seismic isolation systems using the controllable friction damper was analytically confirmed to be as good as, or better than, that of the passive seismic isolation system. The relative displacement of the semi-active seismic isolation systems was less than 60 % of that of the passive seismic isolation system. Moreover, the anticipated effects were achieved with the controllers designed by selecting the weighting coefficients in LQ and IOC theories.

EXCITATION TEST

Test Model and Control System

Verification tests of the semi-active seismic isolation system with the controllable friction damper using the hydraulic system driven by the giant magnetostrictive actuators were conducted with a shaking table.

Figure 13 shows the building test model. The seismic isolation building test model consisted of a superstructure with two steel-frame floors and an isolation story. The total mass of the superstructure was 6,350 kg; the height, the width, and the depth were 2.4 m. The natural period of the isolation system was 3 s, and the rated displacement of the isolation system was ±15 cm. The isolation system consisted of four liner bearings that supported the superstructure, and four coil springs. The controllable friction damper was set up in the center of the isolation story; the rod and the superstructure were jointed; the base plate and the shaking table were jointed. The control system consisted of the DSP, the sensors, and the hydraulic pump driver. The DSP measured the relative displacement between the ground (the shaking table) and the superstructure, and the friction force of the controllable friction damper, and calculated the optimal input with the semi-active control theory. Pressure increases or decreases were judged by the optimal input and the friction force; the pressure increase signal or decrease signal was input to the hydraulic pump driver to control the friction force.

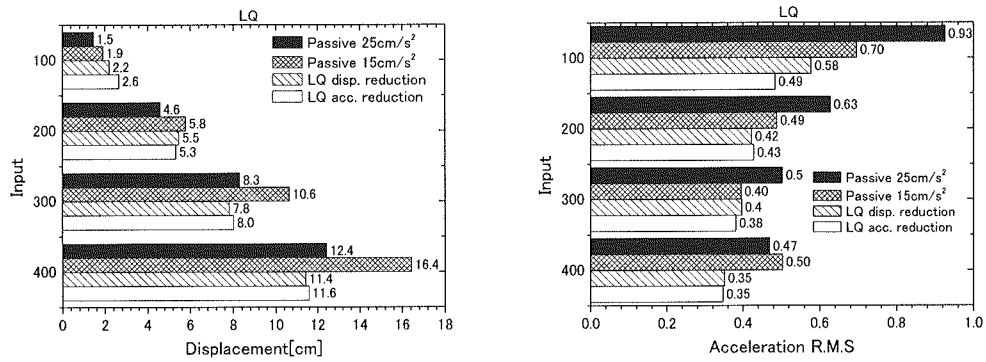

(a) Maximum value of response displacement (b) R.M.S value of response acceleration

Figure 14 Experiment results for LQ

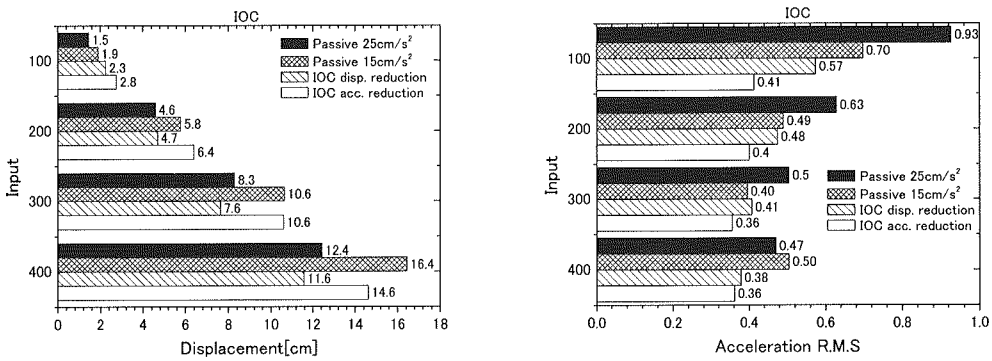

(a) Maximum value of response displacement (b) R.M.S value of response acceleration

Figure 15 Experiment results for IOC

Excitation Test Results

The El Centro NS wave was used as the input in the excitation tests, and the maximum acceleration levels of input wave were set at 100, 200, 300 and 400 cm/s^2. The excitation tests were conducted with the controllers designed for the relative displacement reduction (disp. reduction) and the response acceleration reduction (acc. reduction).

The results of LQ and IOC tests are presented in **Figures 14** and **15**, respectively. Figure (a) presents the maximum relative displacement, and Figure (b) presents the R.M.S. value of the response acceleration, respectively. The results of the passive seismic isolation systems with the constant friction force (passive 15 and 25 cm/s^2 were the cases of the friction force set to begin to slide the friction damper if the input acceleration exceeded 15 and 25 cm/s^2, respectively.) are presented in these figures to compare the performance. The seismic isolation performance of the semi-active seismic isolation systems was better than that of the passive seismic isolation systems, and the relative displacement of semi-active seismic isolation systems became less than that of the passive seismic isolation systems. In the best-case scenario with LQ, the response acceleration was decreased to 53 % compared with that of the passive seismic isolation systems, and the relative displacement was decreased to 70 %. In the best-case scenario with IOC, the response acceleration was decreased to 44 % compared with that of the passive seismic isolation systems, and the relative displacement was decreased to 71 %. Moreover, it was confirmed that the expected performances could be improved with apt design of the semi-active controller.

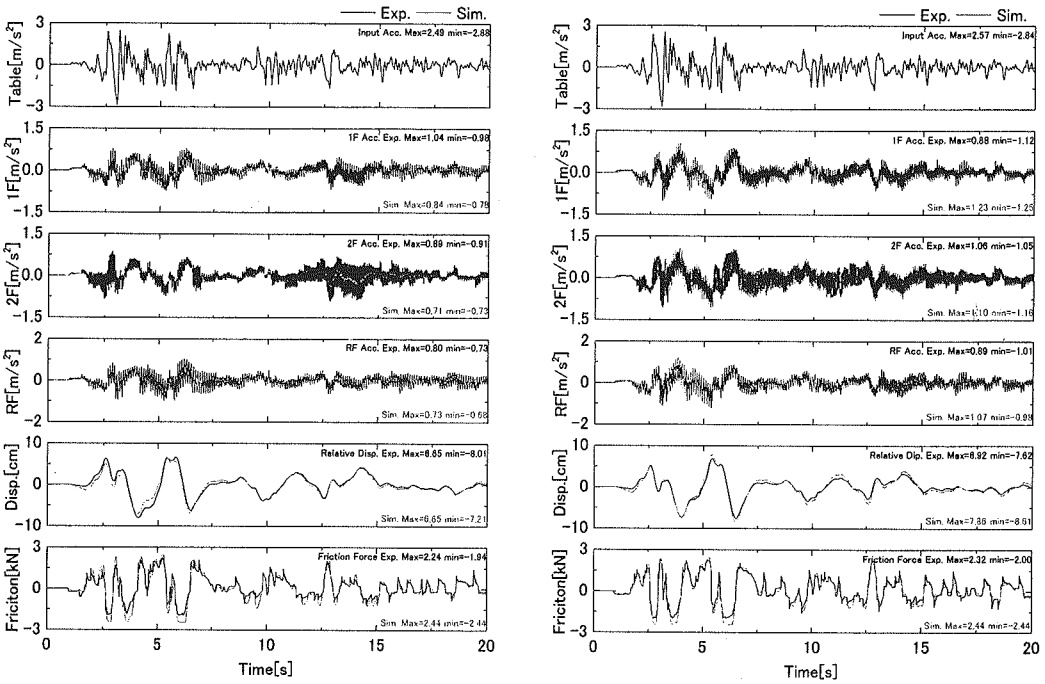

(a) LQ (Acc. reduction) (b) IOC (Acc. reduction)

Figure 16 Time histories of experiment results and simulation results

Finally, numerical simulations were conducted with the three-degree-of-freedom system of the seismic isolation building test model. The time histories of experiment and simulation results with the "acc. reduction" of LQ and IOC are depicted in **Figure 16**. The experiment results contained more high-frequency components, in comparison with those evidences in simulation results. It is assumed that these high-mode excitations occurred because the solenoid valve of the controllable friction damper was abruptly opened or closed and the friction force was turbulent. The simulation results agree with the experiment results if the high-mode excitations are ignored. These results confirmed the validity of the analysis models.

CONCLUSION

A new controllable friction damper for application to large structures was developed. This new controllable friction damper used a hydraulic system driven by giant magnetostrictive actuators, improving the response and operation performance.

Characteristic experiments were conducted with the new controllable friction damper to examine performance. The results confirmed that the new damper performed adequately as the controllable friction damper for a semi-active seismic isolation system; however, the friction force became somewhat turbulent due to the pulse of oil.

Numerical simulations for the semi-active seismic isolation system with the new controllable friction damper were conducted using the analysis model developed based on experiment results. It was analytically confirmed that this semi-active seismic isolation system effectively reduced response acceleration and relative displacement.

Finally, excitation tests for the semi-active seismic isolation system with the new controllable

friction damper were conducted. The results confirmed that the semi-active seismic isolation systems performed better than the passive seismic isolation systems. In addition, the simulation results agreed with the experiment results, confirming the validity of the analysis model. However, the friction force was made turbulent by the abrupt operation of the solenoid valve, so high-frequency modes were excited. Measures to eliminate the turbulence of the friction force will be necessary to apply this new controllable friction damper.

REFERENCES

Sato, E., Fujita, T. (2005). "Semi-Active Seismic Isolation System with Controllable Friction Dampers Using Piezoelectric Actuators" *Transactions of the Japan Society of Mechanical Engineers, Series C*, Vol. 71,No. 702, 405-412.

Murata, Y. et al. (2000). "Development of railway disc brake using giant magnetostrictive material" *Transportation and Logistics Conference*, Vol. 9, 243-246.

Yang, J.N. (1975). "Application of Optimal Control Theory to Civil Engineering Structures" *Journal of Engineering Mechanics Division*, Vol. 101, 819-838